지질학회지 제 58권 제 1호, p. 37-49, (2022년 3월)
J. Geol. Soc. Korea, v. 58, no. 1, p. 37-49, (March 2022)
DOI http://dx.doi.org/10.14770/jgsk.2022.58.1.37

ISSN 0435-4036 (Print)
ISSN 2288-7377 (Online)

남중국해 IODP Site 1432C에서 해양성과 육원성 바이오마커 기록: 과거 40만년간 고해양과 고기후 변동성과의 관련성

현상민[1,‡] · Naokazu Ahagon[2] · Maria Luisa G. Tejada[3] · Mirko Alessandro C. Uy[4] · Alyssa Peleo-Alampay[4] · 김길영[5] · Minoru Ikehara[6]

[1]한국해양과학기술원 해양환경연구센터
[2]Japan Agency for Marine-Earth Science and Technology (JAMSTEC)
[3]Institute for Marine Geodynamics, Japan Agency for Marine-Earth Science and Technology (JAMSTEC)
[4]National Institute of Geological Sciences, University of the Philippines
[5]한국지질자원연구원 해저지질에너지본부
[6]Center for Advanced Marine Core Research, Kochi University

Marine and terrestrial biomarkers records in IODP Site 1432C in the South China Sea: linkage between paleoceanography and paleoclimate variability since the last 400 kyrs

Sangmin Hyun[1,‡] · Naokazu Ahagon[2] · Maria Luisa G. Tejada[3] · Mirko Alessandro C. Uy[4] · Alyssa Peleo-Alampay[4] · Gil-Young Kim[5] · Minoru Ikehara[6]

[1]Marine Environmental Research Center, Korea Institute of Ocean Science and Technology (KIOST), Busan 49111, Republic of Korea
[2]Japan Agency for Marine-Earth Science and Technology (JAMSTEC), Kochi 783-8502, Japan
[3]Institute for Marine Geodynamics, Japan Agency for Marine-Earth Science and Technology (JAMSTEC), Yokosuka-shi Kanagawa 237-006, Japan
[4]National Institute of Geological Sciences, University of the Philippines, Quezon City 1101, Philippines
[5]Marine Geology and Energy Division, Korea Institute of Geoscience and Mineral Resources, Daejeon 34132, Republic of Korea
[6]Center for Advanced Marine Core Research, Kochi University, Kochi 783-8502, Japan

요 약

남중국해 IODP 굴삭지점 U1432C에서 얻어진 시추퇴적물에 대해 알케논과 알칸을 조사하여 과거 40만년간 고해양 변화와 아시아 몬순의 변동성에 대한 관계를 조사했다. 알케논의 평균농도는 0.43 μg/g 이며, 알케논 수온은 22.8~ 27.6°C (평균: 25.86°C; n = 73)으로 빙기-간빙기에 따라 큰 변화를 보인다. 또한, 육원성 바이오마커인 알케인의 농도는 평균 27.92 μg/g이며, 빙기에 증가하고 간빙기에 감소하는 주기적 변화를 보인다. 알케인 지표인 평균 체인길이(ACL)과 CPI (카본지수)는 큰 변화를 보이는데, 아마도 몬순 변화와 따라 바이오마커의 이동 메카니즘의 변화에 기인한 것으로 판단된다. 주기분석의 결과 SST는 4만년 주기의 obliquity (지축경사)를 보임으로써 기후변화와 관계가 있음을 지시한다. 따라서 이 연구는 과거 40만년간의 해양변화가 빙기-간빙기의 주기적 변화를 보이는 반면, 육원성 바이오마커는 아시아 몬순의 영향으로 단주기적 변화를 보이고 있음을 지시한다.

주요어: IODP (국제해저지각시추사업), 남중국해, 알케논, 알케인, 고해양, 동아시아 몬순

‡ Corresponding author: +82-2-51-664-3420, E-mail: smhyun@kiost.ac.kr

ABSTRACT: Two of alkenone and terrestrial *n*-alkane biomarkers derived from the South China Sea (SCS) International Ocean Discovery Program (IODP) 349 sediments were investigated to evaluate the relationship between paleoceanography and Asian monsoon variability since the last 400 ka. The average concentration of total alkenones is 0.43μg/g, and the alkenone-based sea surface temperature (SST_{alk}) ranged from 22.8 to 27.6℃ (average: 25.86℃; n = 73) at studied site U1432C. The concentration of *n*-alkanes shows high fluctuation through the glacial-interglacial periods with average 27.92 μg/g. Indices including average chain length (ACL) and carbon preferences index (CPI) showed large shifts and fluctuations, likely due to differences of delivery mechanism under the East Asian monsoon conditions. Specifically, spectral analysis of SST_{alk} shows a 40-kyr obliquity cycle. Therefore, both alkenone and terrestrial *n*-alkane biomarkers reflect the orbital obliquity cycle, the records of *n*-alkanes are not linearly associated with SST_{alk} paleoceanographic evolution in the last 400 ka. The results of this study suggest that the paleoceanography differs within the glacial-interglacial cycle. However, the terrestrial *n*-alkanes record developed a short-term variation during transportation reflecting paleoclimatic variation in East Asia region.

Key words: IODP, South China Sea (SCS), alkenone, *n*-alkanes, paleoceanography, East Asian Monsoon

1. Introduction

The South China Sea (SCS) is a typical marginal sea. It is connected to the low-latitude Pacific Ocean and encompasses well-preserved hemipelagic sediment that fosters much scientific attention (Fig. 1). SCS sediment reflects the variation in both global glacial-interglacial climatic and local monsoon intensity, as the tropical SCS plays an important role in global climate (Li *et al*., 2004, 2006, 2013; Boulay *et al*., 2005). Many studies have shown that the SCS sediment shows millennial-scale changes in terrestrial sediment input and provide important evidence of a variety of mechanisms involving the strength of East Asian monsoons and migration of the Intertropical Convergence Zone (ITCZ), and their important roles in modulating tropical climate during the glacial and interglacial periods and even Holocene (Lin *et al*., 2006; Wang *et al*., 2016).

Large portions of the sediment within the southern part of the SCS are thought to be delivered from two major neighboring rivers, the Pearl and Mekong Rivers. This means that the sedimentary record in the SCS may reflect direct inputs from these rivers, including terrestrial materials and other geological proxies that can be used to understand terrestrial environmental changes (Boulay *et al*., 2005; Liu *et al*., 2010; Zhou *et al*., 2012). In addition to this direct inputs, sediment is thought to be transported by atmospheric circulation that depends on the intensity of monsoons that occur within continental Asia (Wang

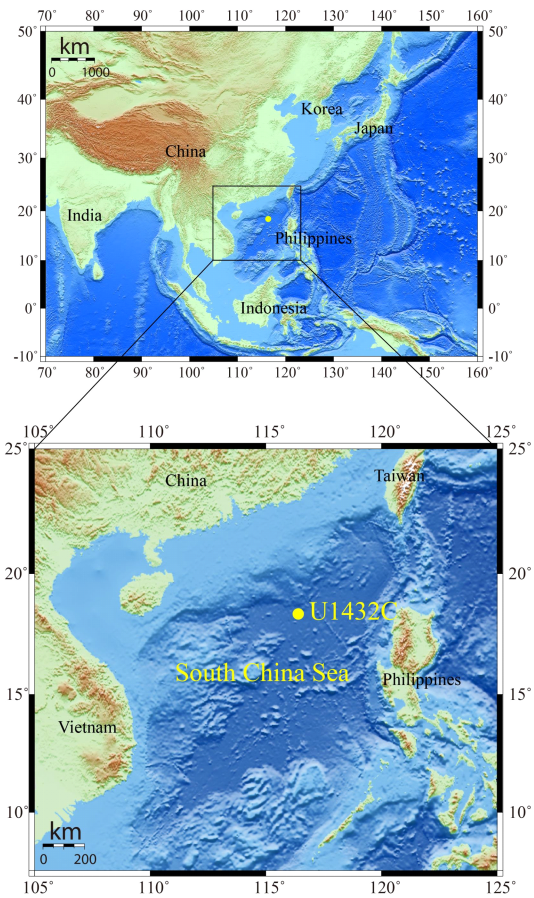

Fig. 1. Physiographic map of the South China Sea (SCS) and surrounding areas (upper) and the locations of U1432C (lower).

and Li, 2009). Therefore, sedimentary records of the SCS reflect both paleoceanographic and paleoclimatic changes that include South East Asian monsoon intensity (Lin *et al*., 2006; Zhao *et al*., 2006; Wang and Li, 2009; Wang *et al*., 2014).

Two bio-proxies have been used to evaluate the linkage between paleoceanographic and paleoclimatic variability in the SCS and Asian continent. For this, alkenones have been used most widely to reconstruct past sea surface temperature (SST), which is directly related to climatic change in the SCS (Pelejero and Grimalt, 1997; Pelejero *et al*., 1999a, 1999b; Mercer and Zhao, 2004; Zhao *et al*., 2006). Fluctuations in alkenone-based SST (SST_{alk}) were initially reported for SCS sediments corresponding to glacial and interglacial periods (Pelejero *et al*., 1999a), where subsequent studies have connected such changes to both global climatic changes and monsoon variability (Pelejero, 2003; Wang *et al*., 2014). The second one, terrestrial biomarker *n*-alkane has also been studied in the SCS to understand hydro-climatic changes (Pelejero, 2003; Hu *et al*., 2009; Zhou *et al*., 2012; Li *et al*., 2013, 2015b, 2015c). Therefore, alkenones and n-alkanes have both been used to understand the input of terrestrial proxies as paleovegetation changes, and so paleoclimate variation and their relationship in this study area (Sun *et al*., 2000; Pelejero, 2003; Hu *et al*., 2009; Li *et al*., 2011, 2013; Wang *et al*., 2014).

In terms of the importance of the SCS for understanding the linkage between the paleoceanography of the SCS and paleoclimate variability in East Asia, many studies have shown a major effect of the SCS on variability in the Asian monsoon intensity, as well as global ocean changes (Wan *et al*., 2006; Li *et al*., 2015c). For example, variation in the SST of the SCS is synchronous with Greenland warming during deglaciation (Kienast *et al*., 2001; Zhao *et al.*, 2006) and the paleoceanography of the SCS should be associated with eustatic sea-level changes, the carbon reservoir, and with the paleoceanographic conditions of the western Pacific warm pool in global scale (Li *et al*., 2006; Wang *et al*., 2014). However, terrestrial inputs represented by *n*-alkanes and a comparison with paleoceanographic evolution and latitudinal differences were not fully discussed in these previous works. In this study, we reconstructed the past SST_{alk} and *n*-alkane concentrations in the SCS as they relate to variation in the East Asian monsoon intensity and SCS paleocealography during the last 400 ka. We used newly established chronostratigraphy to reconstruct these purposes, which provide insight into paleoceanographic variation and its relationship with paleoclimatc variability in the southern and northern SCS.

2. Materials and methods

The International Ocean Discovery Program (IODP) Expedition 349 site U1432C used in this study is located at 18°21.0831′N, 116°23.4504′E (water depth: 3,829 m) in the north part of the SCS (Fig. 1). Sediments from this site are composed of clay, silt and sand (Fig. 2). All the the samples used for the alkenones and n-alkanes were collected on-board and then analyzed at the KIOST.

For the alkenones and *n*-alkanes analyses, lipids were extracted (x 3) from 5 g of dried sediment using a DIONEX-Accelerated Solvent Extractor ASE-200 at 100°C and 1000 psi for 10 min with 11 ml of CH_2Cl_2-CH_3OH (6:4) and then concentrated. The lipid extract was separated into four fractions using column chromatography (SiO_2 with 5% distilled water; i.d., 5.5 mm; length, 45 mm): F1 (hydrocarbons), 3ml hexane; F2 (aromatic hydrocarbons), 3 ml hexane-toluene (3:1); F3 (ketones), 4 ml toluene; F4 (polar compounds), 3 ml toluene-CH_3OH (3:1); n-$C_{36}H_{74}$ was added as an internal standard to F3.

Gas chromatography (GC) for the analysis of alkenones and *n*-alkanes in the F3 and F1 fractions were conducted using a Hewlett Packard 5890 series II gas chromatography with on-column injection and electronic pressure control systems, and a flame ionization detector (FID). Samples were dissolved

in hexane. Helium was the carrier gas and the flow velocity was maintained at 30 cm/s. A Chrompack CP-Sil$_5$CB column was used (length, 60 m; i.d., 0.25 mm; thickness, 0.25 μm). The oven temperature was programmed to rise from 70 to 290°C at 20°C/min, from 290 to 310°C at 0.5°C/min, and to hold at 310°C for 30 min. Prior to quantification of lipids, a known aliquot of an internal standard, 5α-Cholestane (Sigma Aldrich), was added to the hydrocarbon fraction. The compound peak areas were normalized to those of the internal standards and converted to mass quantities using response curves for about 18 hydrocarbon standard compounds (Hydrocarbon Window Defining Standard, AccuStandard) analyzed in concentrations ranging from 10 to 200 μg/ml. The standard deviations of three duplicate analyses averaged 7.5% of the concentration for each compound. Peaks of *n*-alkanes and alkenones were identified by gas chromatographic retention times by analogy with synthetic standards. The concentrations of both compounds were calculated by comparing their peak areas to those of the internal standard.

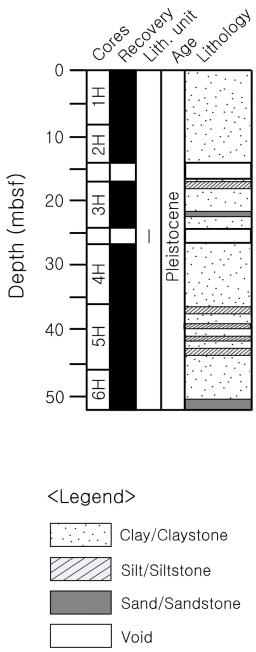

Fig. 2. Simplified lithology of U1432C and the analysis intervals are drawn only.

Alkenone unsaturation index UK'_{37} was calculated from the concentrations of di- and tri-unsaturated C_{37} alken-2-ones [C37MK] using the following expression (Prahl and Wakeham, 1987; Prahl *et al*., 1988): $UK'_{37} = [C_{37:2}MK]/([C_{37:2}MK] + [C_{37:3}MK])$. Temperature was calculated according to the equation: $UK'_{37} = 0.031T + 0.092$, where T = temperature [°C] based on previous results from the SCS (Pelejero and Grimalt, 1997). Analytical accuracy was 0.24°C in laboratory condition.

3. Results and discussions

3.1 Lithostratigraphy and age model

To understand the details of paleoceanographic variation and its relationship to variability of the East Asian monsoon, it is first necessary to reconstruct a reliable sedimentary lithostratigraphy. Sediment from Site U1432C from northern South China Sea (northern SCS) is composed mainly of clay, with minor contributions of silt and sand, with intermittent turbidite layers (Fig. 2). The lithostratigraphic unit of the studied site was defined as only one unit, implying that U1432C (northern SCS) the sediment of this site has not significant variation. Sediments were only taken from 0 to 51.3 mbsf in U1432C (Li *et al*., 2015a) (Table 1). A simplified lithostratigraphy was constructed based on onboard sedimentological characteristics, biostratigraphic data and magnetostratigraphy, and used in this study (Fig. 2).

Based on the on-board measurement, the age of the bottom in U1432C (110 mbsf) is less than 0.91 Ma; characterized by marine microfossil, occurs at the B/M boundary, which corresponds to 105 mbsf (0.781 Ma). Additionally, the average sedimentation rate of ~12 cm/ky does not vary within the sediment column (Li *et al*., 2015a). However, the samples used in this study do not not cover the whole age span. Only samples from the upper part (present to 400 kyrs) were used due to the absence of continuous samples (Fig. 2, 3). The average sedimentation

Table 1. Comparison of alkenone concentration and n-alkane data with several references.

Site and Reference	Latitude	Longtitude	Water Depth (m)	Penetration DSF (m)		Alkenones (μg/g)	SST	*n*-Alkanes (μg/g)	ACL	CPI
U1432C	18°21.0831'N	116°23.4504'E	3829.0	51.3 (110.0)	Max	2.75	27.58	155.45	30.28	4.15
					Min	0.03	22.77	6.01	28.22	0.79
					Avg	0.43	25.86	27.92	29.19	2.20
Harada *et al*. (2006)	Okhotsk Sea				Max	0.59*	16.2*			
					Min	0.21*	5.0*			
Hyun *et al*. (2013)	East Sea				Max	15.15	18.27			
					Min	0.25	6.64			
					Avg	3.91	12.84			
Li *et al*. (2013)	South China Sea				Max		29.5*	0.84*	28.0*	1.0*
					Min		24.9*	0.09*	30.8*	4.0*
Hu *et al*. (2009)	South China Sea				Max			2.50*		
					Min			0.68*		
					Avg			1.32*		

( ) is cored interval, * indicates that the values came from the graphic data.

rates were approximately ~12.1 cm/kyr. This relatively high sedimentation rate makes it possible to compare with the past changes in SCS.

3.2 Alkenone concentration, alkenone-based SST (SST_{alk})

The total alkenone C_{37} contents of sediment from the studied sites are highly variable. The total alkenone C_{37} concentration (μg/g) ranged from 0.03 to 2.75 μg/g (average: 0.43 μg/g; n = 73) and varies among different sampling depth with a great degree of fluctuation (Fig. 4). However, it is characterized by a striking drop at several layers, with low concentrations. Entirely, total C_{37} alkenone contents for this site is similar to those from the Okhotsk Sea (Harada *at al*., 2008) and the East Sea of Korea (Lee *et al*., 2008; Hyun *et al*., 2013) (Table 1). Also, values in total C_{37} alkenones are similar to previous results from the SCS (Pelejero *et al*., 1999a; Zhao *et al*., 2006), suggesting that the total C_{37} alkenone concentrations are reasonable and are reliable proxies for the reconstruction of paleoenvironmental changes in SCS.

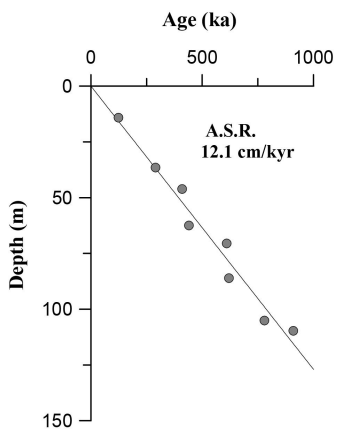

Fig. 3. Age model for this site. Original data and each age control points were from the model defined by Li *et al*. (2015a). A.R.S is average sedimentation rate.

The concentration of total alkenones can be attributed to different population densities of *Emiliania huxleyi* and *Gephyrocapsa oceanica* in ocean. Haptophyte microalgae usually produce a particular class of lipid, long-chain unsaturated ketones, in specific environments, although the exact synthetic mechanism is also associated with factors including nutrients levels, water temperature, and other physical conditions. The total C_{37} alkenones comprise $C_{37:2}$, $C_{37:3}$, and $C_{37:4}$, which are expressed as di-($C_{37:2}$), tri-($C_{37:3}$), and tetra-unsaturated ($C_{37:4}$) members. Among these three compounds, $C_{37:4}$ ($C_{37:4}$%) was not detected

in this study, even though its presence in natural and cultured samples has been reported previously (Sikes *et al*., 1997; Sicre *et al*., 2002). The absence of certain coccolith species may result in the absence of $C_{37:4}$ in the SCS. *G. oceanica* is probably more likely to produce alkenones in the SCS. Therefore, the paleoceanographic conditions within the SCS for producing C_{37} alkenones may differ from other oceanographic conditions. One study also reported the absence of $C_{37:4}$ alkenones in the southern SCS (ODP Leg 184) (Mercer and Zhao, 2004). This suggests that oceanographic conditions were not favorable for $C_{37:4}$ alkenone synthesis, where such oceanographic conditions could differ from other oceans since production initiation at approximately 31 Ma (Pelejero *et al*., 1999b; Mercer and Zhao, 2004).

The alkenone-based SST_{alk} variations in this study range from 22.8-27.6℃ (average: 25.86℃; n = 73). Previous studies that investigated changes in

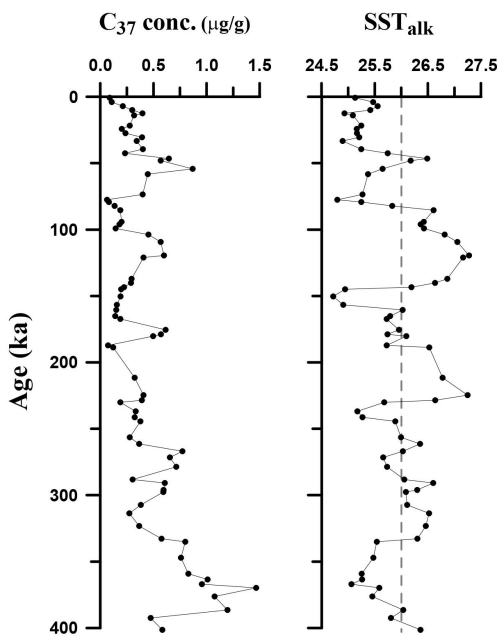

Fig. 4. The total alkenone concentration (C_{37}) and alkenone-based sea surface temperature (SST_{alk}) in studied Site. The SST_{alk} reconstructed using the formulae of Pelejero and Grimalt (1997) is given. All points are three-point moving averages.

SST differences during the Pleistocene found that the difference in SST_{alk} was as much as 4℃ during the last 1.0 Ma, with distinct glacial-interglacial fluctuation, and it became lower by as much as about 1℃ around 2.0 Ma (Herbert *et al*. 2010). The most important characteristic of sedimentary records for constructing SST_{alk} records is the glacial-interglacial cyclic fluctuation in SCS (Li *et al*., 2011; Wang *et al*., 2014). In particular, alkenone-related proxies also show that the SST_{alk} in the SCS remains steady at ~29℃, noting fluctuations of <1℃ before 2.7 Ma, followed by strong oscillations after this time (Li *et al*., 2011). The SST_{alk} generally showed fluctuations on a millennial scale and was strongly associated with monsoons during the more recent late Pleistocene period (Pelejero *et al*., 1999a; Zhao *et al*., 2006). Similarly, the SST_{alk} determined in this study appears to have varied cyclically since approximately 400 ky (Fig. 4). This means that paleoceanographic conditions over the last 400 ka reflect the global glacial-interglacial regime.

The SST_{alk} differences are dominated by glaciers, indicating strengthening during glaciation and weakening during winter monsoons in interglacial periods (Wang *et al*., 2014). Therefore, the SST_{alk} fluctuation during glacial-interglacial in SCS may be linked to the global evolution of paleoclimate conditions. Larger fluctuation between wet and dry conditions occurring since 1 Ma, as shown by terrestrial *n*-alkane biomarker, may be associated with neighboring continental paleoclimatology (Li *et al*., 2013).

3.3 *n*-alkane concentration, and its variation and sources

In general, *n*-alkanes derived from epicuticular leaf waxes are dominated by long, odd-numbered alkanes within the nC_{24}-nC_{35} range (Eglinton and Eglinton, 2008). Because high-molecular-weight *n*-alkanes such as nC_{29} and nC_{31} mainly come from higher land plants, the total *n*-alkane concentration is usually used to indicate the predominance of paleo-vegetation species and the abundance of land-

derived plants (Li *et al*., 2013). These long-chain *n*-alkanes are easily transported from land to the ocean, where their abundance and variability may reflect variation in the plant communities within the source areas. Therefore, *n*-alkane predominance and its distribution can be used to determine the type of higher plant, and thus useful for tracking environmental changes (Sikes *et al*., 2009; Ahad *et al*., 2011).

In this study, the concentration of total *n*-alkanes (nC_{25}~nC_{35}) varied widely, and showed time-dependent variation in individual *n*-alkane components in this site (Fig. 5, 6; Table 1). There was a predominance of odd-numbered compounds, but this distribution included an exceptional distribution, as seen in a sample from the 190~230 ka (Fig. 7). This exceptional event is consistent with an extremely high *n*-alkane concentration, as much as two to five times higher than those of other intervals (Fig. 5). Considering that an odd-numbered distribution is a distinct characteristic of the *n*-alkane distribution, this exceptional case is interpreted as being influenced by different sources of vegetation or plant communities.

As nC_{31} is derived from grassland plants and nC_{27} from forest trees and shrubs (Li *et al*., 2013), high nC_{31}/nC_{27} ratio is used to detect dry conditions

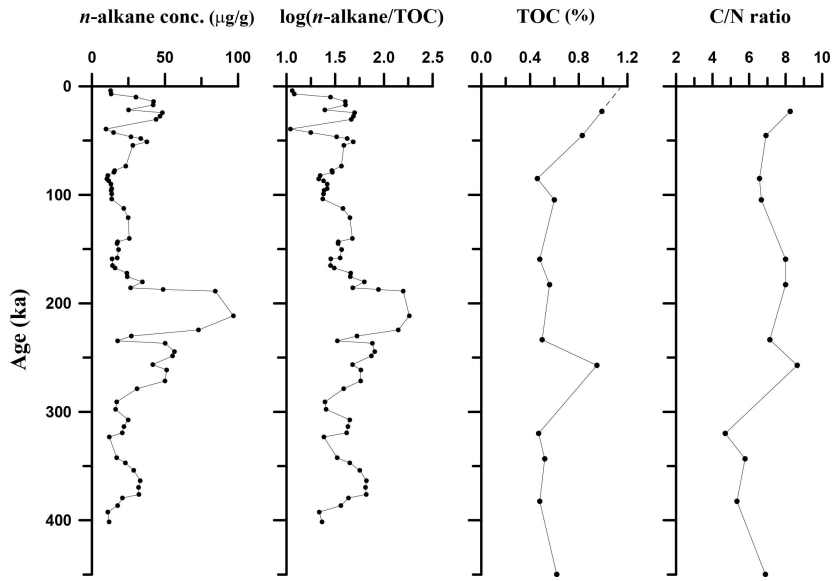

Fig. 5. The time-dependence of total *n*-alkane concentrations and n-alkane/TOC. TOC (%) and C/N ratios were referred from initial report of IODP (Li *et al*., 2015a). All points are three-point moving averages.

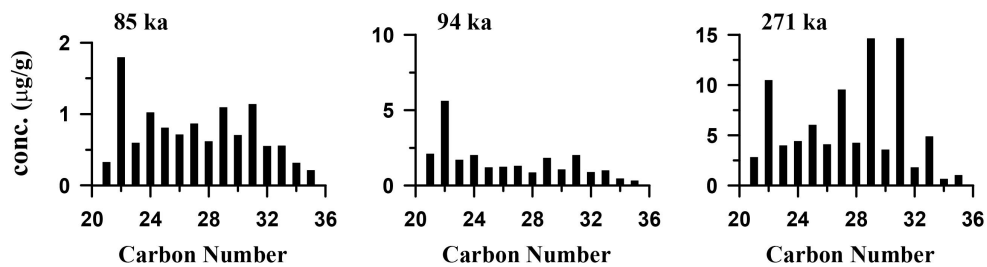

Fig. 6. Three representative *n*-alkane distributions are illustrated. The *n*-alkane distribution clearly differed over time, suggesting paleovegetation changes in the source area.

during glaciation, where lower values occur during wetter conditions in interglacial periods. As shown in Fig. 7, nC_{31}/nC_{27} fluctuated between approximately 1 and 3, which is similar to the SCS sediment records obtained by Li *et al*., (2013). Given this information, nC_{31}/nC_{27} is useful for detecting shifts in hydroclimate conditions within source areas, the rough lowering trend observed between 400 ka and 210 ka, and 190 ka and present may attribute to periodic warming and gradual wetting condition, long-range paleoclimatic variation. These fluctuations may contribute to glacial-interglacial cycles or long-term climatic changes in East Asia; note that this may also be due to paleovegetation changes in source areas. As mentioned, high-molecular-weight *n*-alkanes (nC_{27} and nC_{31}) derived from epicuticular leaf waxes (higher plants), and can be easily transported into oceans, even over long distances (Yokoyama *et al*., 2006; Hu *et al*., 2009). Therefore, both nC_{27} and nC_{31} appearing in studied sediment are useful for detecting past variation in the paleovegetation and paleoclimate of source areas. In particular, periodic long-term lowing in nC_{31}/nC_{27} may imply gradual warming and wetting paleoclimatic variability in East Asian continent. Instead, distinctive decrease in nC_{31}/nC_{27} could be observed at around 10 ka, 110 ka and 220 ka (arrows in Fig. 7) indicating 100 ka cyclic short-term wet condition.

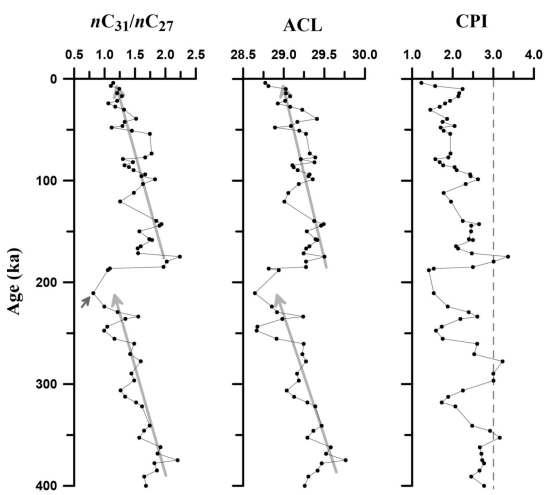

Fig. 7. Vertical profiles of nC_{31}/nC_{27}, average chain length (ACL) and carbon preference index (CPI) in studied site, suggesting dry conditions when the ratio was high and *vice versa*. Clear lowering patterns of this ratio were recognized in two intervals; approximately from 380 ka to 210 ka, and from 180 ka to present (two arrows) implying long-term paleoclimatic variability.

The ACL is defined by the average chain length of *n*-alkanes derived from higher terrestrial plants. It usually refers to the average number of carbon atoms per molecule and provides insight into the variability in alkane distribution. Changes in ACL are therefore strongly associated with the temperature and aridity of the plant growing environment (Collister *et al*., 1994). This means that the leaf wax chain length can change to protect plants by minimizing water evaporation. Therefore, it is possible to delineate possible *n*-alkane sources by identifying environmental differences, even though the usefulness of this approach is limited only to source-specific *n*-alkane distribution (Jeng, 2006).

We showed that ACL fluctuated widely throughout with significant differences. In particular, about 200 ka range gradual decrerase of ACL is quite similar with the excursion of nC_{31}/nC_{27}, which indicates that paleovegetation changes are further related to local climatic changes (Fig. 7). Therefore, changes that occurred around 210 ka imply diverse plant communities due to changes in latitude or supply differences due to paleoclimate variation. An intermittent increase in ACL around 370 ka may indicate a temporal increase in merged C_3 plants. This pattern can be interpreted as indicating variation in the plant population throughout the entire interval, further indicating broad paleoclimatic variation. Pelejero (2003) used Quaternary sediment from SCS ODP Site 1143 to show that the ACL of *n*-alkanes varies from 29 to 31, which is consistent with our result and with another study in the same area (Li *et al*., 2013) (Fig. 7). In addition to ACL, carbon preference index (CPI) originating from terrestrial plant waxes also provides valuable information regarding the *n*-alkane source (Bi *et al*., 2005). Terrestrial plant wax-

es generally have high CPI (>3), whereas lower CPI is reflective of short-chain *n*-alkane distribution. In our study, CPI values fluctuated widely and ranged from 1.0 to 4.0 (Fig. 7).

Previously, Li *et al*., (2013) attributed CPI variation (specifically within lower values of CPI) to the following four reasons: 1) petroleum intermixture, 2) post-depositional alterations, 3) older detrital intermixture, and 4) marine algal response. In the case of petroleum sources, petrogenic hydrocarbons generally reduce the final CPI in sediment (Seki *et al*., 2004; Jeng, 2006). The *n*-alkanes in petrogenic sources, such as crude oil and high rank coal, generally do not show a preference for odd-carbon numbers, and tend to have high concentrations in the nC_{15}-nC_{25} range (Petersen *et al*., 2007). This implies that their sources can be modeled using a simple two end-member model (Ishiwatari *et al*., 1994; Street *et al*., 2013), and supports that most *n*-alkanes are supplied from terrestrial leaf waxes. Therefore, the molecular composition of lipid biomarkers provides important proxies for discriminating source materials (Nott *et al*., 2000; Yokoyama *et al*., 2006; Yamamoto *et al*., 2010). In our data, CPI values are generally greater than 1; therefore, long-term admixture in marine settings is not possible, and degradation by microbial activity might eliminate previous carbon ratios in alkanes. Older detrital matter intermixtures and marine algal response during the Pleistocene interglacial period may have also reduced the CPI. As a consequence, all of these factors could have altered the CPI. However, their influence on the high molecular weight and odd carbon ratios observed is minor (Zhou *et al*., 2012; Li *et al*., 2013).

3.4 Paleoceanography and its relationship with East Asian Monsoon variability

3.4.1 Alkenones

The concentration of total alkenones within the SCS sediments shows significant variability in terms of its age and location (Mercer and Zhao, 2004; Boulay *et al*., 2005). Specifically, alkenone compounds may have been synthesized during the last 31 Ma, when low latitude Pacific Ocean water inflows into the SCS dominated primitive SCS paleoceanography. In present study, alkenone $C_{37:4}$ is not found in the SCS as reported previously (Pelejero and Grimalt, 1997), although alkenones $C_{37:2}$, $C_{37:3}$, and $C_{37:4}$ were present in similar marginal basins such as the East Sea (Fujine *et al*., 2009; Hyun *et al*., 2013) and Okhotsk Sea (Harada *et al*., 2006, 2008).

The concentration of total alkenones and the corresponding initiation of alkenone synthesis are thought to be associated with long-range paleoceanography evolution in the SCS. As discussed earlier, SST_{alk} in this study ranged from 22.8-27.6°C, approximately corresponding to previous studies (Pelejero *et al*., 1999a; Zhao *et al*., 2006); specifically, SCS from ODP Site 1143, Site 1146 (Herbert *et al*., 2010). Therefore, our results reflect the SCS SST_{alk} well and may coincide with global SST_{alk} variation throughout the last 400 ka (Table 1).

To understand the relationship between SST_{alk} and indices of *n*-alkanes as a proxy of paleoclimatic variation, we performed a spectral analysis spanning the last 400 ka. A dominant power at the obliquity band (ca. 0.024 cycles/kyr) was observed in SST_{alk}, as shown in Fig. 8. Previous studies determined long-term terrestrial cycles within the Loess Plateau in China, in which a Quaternary ocean cycle occurred in ~400 kyr rhythms that was ascribed to long eccentricity in orbital forcing (Wang *et al*., 2014). Generally, it is true that orbital cycles are a prominent feature in SST_{alk} in the SCS, where previous works show long-term cyclic variation based on SST_{alk} and foraminiferal variation based on transfer functions (Wang *et al*., 2014).

Several methods such as foraminiferal transfer function and a stable isotope study of foraminifera have shown the SST variation for the last 2 Ma, and have been compared with each other (Wang *et al*., 2014 and references therein), which show global-scale variation over the last 2 Ma. Likewise, this study reconstructed the glacial-interglacial fluctua-

tion of SST_{alk} for the last 400 ka using biomarker studies, and the spectral analysis results in clear obliquity and precession cycles. Considering these SST variations in previous studies, the SST_{alk} variation during glacial-interglacial periods also reflects global and regional variation in solar energy, demonstrating climatic influences and reflect possible variation in the East Asian monsoons.

3.4.2 *n*-alkanes

Long-term changes in paleoceanographic conditions in the SCS have been associated with Asian tectonic events, noting much long-term variation (Li *et al*., 2006). One of the best examples of the relationship between tectonic and paleoceanography evolution was by Li *et al*. (2006). Specifically, changes in the SCS have been linked to SCS rifting, spreading, and monsoon influence since 33 Ma, where the prevalence of glaciers characterized the last 5-0 Ma. This implies that sediment supplied by river influx, as well as atmospheric influences such as aeolian dust, contributed to long-term paleoclimatic variation. Indeed, our data show long-range fluctuation in *n*-alkane total concentration, with gradual change. The total concentration of total *n*-alkanes may be related to several mechanisms, including the degree of synthesis within the source area and its transportation and biodegradation. As we discussed earlier, total *n*-alkane concentration shows considerable fluctuation over time, with significant increases around 180 and 380 ka. These abrupt increase in *n*-alkanes in these intervals may be attributed to a climatic event observed by SST_{alk} at this site.

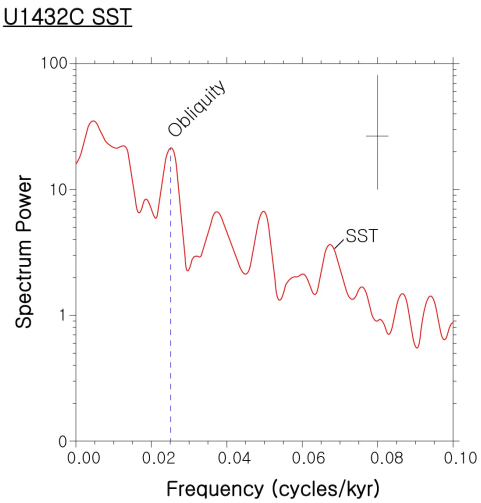

Fig. 8. Spectral analysis of SST_{alk} and *n*-alkanes. Orbital cycles (possible obliquity) can be recognized in SST_{alk} at site U1432C.

As discussed previously, *n*-alkane distribution can be assessed in terms of paleovegetation extent, and is used therefore to estimate the climatic conditions of the source area. A representative ACL index can differentiate between arid and/or wet conditions by chain length, as shown in Li *et al*. (2015c). Because ACL is concentration-weighted, and comprised mainly of C_{27}, C_{29} and C_{31} *n*-alkanes, variation in ACL is commonly associated with changes in temperature and aridity of the growing environment of plants (Poynter *et al*., 1989). As shown in Fig. 7, C_{31}/C_{27} shows drastic variation, which are roughly coincident with ACL variation. These proxies imply paleoclimate variation within East Asia and may influence paleoceanographic variation as their flux can be detected in sediment records.

To better understand the relationship between *n*-alkane flux and SST_{alk} in this study, spectral analysis was conducted over the last 400 ka. The spectral analysis for *n*-alkanes did not show any patterns, which may indicate that *n*-alkane concentration is influenced by multiple variables beyond climatic factors. For example, lithogenic input such as clay minerals can dilute organic matter, and *n*-alkane concentration also decreases exponentially over time (Boulay *et al*., 2005). As discussed earlier, the orbital cycles in both SST_{alk} and each compound or indices analyzed do not show consistent patterns, whereas SST_{alk} shows 40 kyr obliquity like orbital cycle.

Concerning the relationship between *n*-alkane input and SST_{alk}, the *n*-alkane concentration appears to maintain an inverse relationship with SST_{alk} in

SCS sediment (Pelejero, 2003). This study revealed that the pattern of glacial to interglacial variability of the *n*-alkane concentration is parallel, and it shows a linear inverse relationship to the SST_{alk}, with high concentrations during cold glacial intervals and low ones during warm interglacial periods. They interpreted this inverse relationship and terrestrial markers as being due to emergence and flooding of the shelves due to sea-level variation. The comparison between SST_{alk} and total *n*-alkane concentration in our study seems to suggest an inverse relationship, although linear curve fitting was not conducted. Therefore, given that SST_{alk} is a proxy of paleoceanographic variation, the high fluctuation in the *n*-alkane concentration and its inverse relationship might be associated with the paleoclimatic variation in East Asia, and this is recorded in SCS sediments.

4. Conclusions

Sediments collected from the IODP Exp. 349 site within the SCS were investigated to understand paleoceanographic variation and paleoclimatic variability, specifically the relationship between these two factors over the last 400 ka. The marine biomarkers, alkenones concentrations, and alkenone-derived SST_{alk} delineate striking temporal differences. The SST_{alk} exhibited orbital cyclic variation during the last 400 ka. Estimated SST_{alk} ranged from 22.8-27.6°C (average: 25.86°C; n = 76), reflecting glacial-interglacial variation.

The concentrations of *n*-alkanes (nC_{25-35}) show high fluctuation. The average chain length (ACL) and carbon preference index (CPI) showed large shifts and fluctuations in terrestrial organic compounds. Several terrestrial biomarker indices (such as ACL and CPI) indicated long-term variation, hinting to large variation in SCS paleoceanography in conjunction with paleoclimatic variation in East Asia. The inverse relationship between SST_{alk} and the influx of *n*-alkanes supports the association of a high flux of *n*-alkane with cold and arid conditions, and low SST_{alk} in paleoceanographic conditions in the SCS.

Spectral analysis of SST_{alk} shows orbital cycle with high spectrum power; however, the results for the proxies of *n*-alkanes do not match with those of SST_{alk}. Therefore, paleoceanographic variation and the influx of terrestrial organic biomarkers are associated with the paleoclimatic variation in SCS. In particular, the variability in the East Asian monsoon has been influenced on the variations of paleoceanography. Differences in SST_{alk} and *n*-alkane concentration in this site may be linked to paleoceanographic conditions as well as changes in Asian monsoon intensity over the last 400 ka.

Acknowledgement

This research used samples and/or provided data by the International Ocean Discovery Program (IODP). Funding for this research was provided by the K-IODP (PM62120), which was funded by Ministry of Ocean and Fisheries, Korea. We thank the two reviewers for their helpful comments and crews of South China Sea Exp 349. This study was supported by the KIOST program (PE99775) in part.

REFERENCES

Ahad, J.M.E., Ganesharm, R.S., Bryant, C.L., Cisneros-Dozal, L.M., Ascough, P.A., Fallick, A.E. and Slater, G.F., 2011, Sources of n-alkanes in an urbanized estuary: insights from moleular distributions and compound-specific stabl and radiocarbon isotopes. Marine Chemistry, 126, 239-249.

Bi, X., Sheng, G., Liu, X., Li, C. and Fu, J., 2005, Molecular and carbon hydrogen isotope composition of n-alkanes in plant leaf waxes. Organic Geochemistry, 36, 1405-1417.

Boulay, S., Colin, C., Trentesaux, A., Frank, N. and Liu, Z., 2005, Sediment sources and East Asian monsoon intensity over the last 450 ky. Mineralogical and geochemical investigations of South China Sea sediments. Paleogeography, Paleoclimatology, Paleoecology, 228, 260-277.

Collister, J.W., Rieley, G., Stern, B., Eglinton, G. and Fry, B., 1994, Compound-specific $\delta^{13}C$ analyses of leaf lipids from plant with differing carbon dioxide metabolisms. Organic Geochemistry, 21, 619-627.

Eglinton, T.I. and Eglinton, G., 2008, Molecular proxies for paleoclimatology. Earth and Planetary Science Letter, 275, 1-16.

Fujine, K., Tada, R. and Yamamoto, M., 2009, Paleotemperature response to monsoon activity in the Japan Sea during the last 160 kyr. Paleogeography, Paleoclimatology, Paleoecology, 280, 350-360.

Harada, N., Ahagon, N., Sakamoto, T., Uchida, M., Ikehara, M. and Shibata, Y., 2006, Rapid fluctuation of alkenone temperature in the southwestern Okhotsk Sea during the past 120 ky. Global and Planet Changes, 53, 29-46

Harada, N., Sato, M. and Sakamoto, T., 2008, Freshwater impacts recorded in tetraunsaturated alkenones and alkenone sea surface temperatures from the Okhotsk Sea across millennial-scale cycles. Paleoceanography, 23, https://doi.org/10.1029/2006PA001410.

Herbert, T.D., Peterson, L.C., Lawrence, K.T. and Liu, Z., 2010, Tropical ocean temperature over the past 3.5 million years. Science 328:1530-1534

Hu, J., Peng, P. and Chivas, A.R., 2009, Molecular biomarker evidence of origins and transport of organic matter in sediments of the Pearl River estuary and adjacent South China Sea. Applied Geochemistry, 24, 1666-1676.

Hyun, S., Kim, J.M., Yim, U.H., Shim, W.J., Yoon, S.H. and Woo, K.S., 2013, Variations in sea surface temperatures based on alkenones in Korea Plateau sediments of the East Sea (Sea of Japan) over the last 300,000 years. Journal of Asian Earth Science, 66, 140-149.

Ishiwatari, R., Uzaki, M. and Yamada, K., 1994, Carbon isotope composition of individual *n*-alkanes in recent sediments. Organic Geochemistry, 21, 801-808.

Jeng, W.L., 2006, Higher plant n-alkanes average chain length as an indicator of petrogenic hydrocarbon contamination in marine sediments. Marine Chemistry, 102, 242-251.

Kienast, M., Steinke, S., Stattegger, K. and Calvert, S.E., 2001, Synchronous tropical South China Sea SST change and Greenland warming during deglaciation. Science, 291, 2132-2134.

Lee, K.E., Bahk, J.J. and Choi, J., 2008, Alkenone temperature estimates for the East Sea during the last 190,000 years. Organic Geochemistry, 39, 741-753.

Li, B., Wang, J., Huang, B., Li, Q., Jian, Z., Zhao, Q., Su, X. and Wang, P., 2004, South China Sea surface water evolution over the last 12 Myr: A south-north comparison from Ocean Drilling Program Sites 1143 and 1146. Paleoceanography, 19, PA1009, https://doi.org/1029/2003PA0000906.

Li, C.-F., Lin, J., Kulhanek, D.K. and the Expedition 349 Scientists, 2015a, South China Sea Tectonics: Proceedings of the International Ocean Discovery Program Proceedings of the International Ocean Discovery Program Volume 349, https://doi.org/10.14379/iodp.proc.349.104.2015.

Li, L., Li, Q., He, J., Wang, H., Ruan, Y. and Li, J., 2015b, Biomarker-derived phytoplankton community for summer monsoon reconstruction in the western South China Sea over the past 450 ka. Deep-Sea Research II, 122, 118-130.

Li, L., Li, Q., Li, J., Wang, H., Dong, L., Huang, Y. and Wang, P., 2015c, A hydroclimate regime shift around 270 ka in the western tropical Pacific inferred from a late Quaternary *n*-alkane chain-length record. Paleogeography, paleoclimatology, Paleoecology, 427, 79-88.

Li, L., Li, Q., Tian, J., Wang, H. and Wang, P., 2013, Low latitude hydro-climatic changes during the Plio-Pleistocene evidence from high resolution alkane records in the southern South China Sea. Quaternary Science Review, 78, 209-224.

Li, L., Li, Q., Tian, J., Wang, P., Wang, H. and Liu, Z., 2011, A 4-Ma record of thermal evolution in the tropical western Pacific and its implications on climate change. Earth and Planetary Science Letter, 309, 10-20.

Li, Q., Wang, P., Zhao, Q., Shao, L., Zhong, G., Tian, J., Cheng, X., Jian, Z. and Su, X., 2006, A 33 Ma lithostratigraphic records of tectonic and paleoceanographic evolution of the South China Sea. Marine Geology, 230, 217-235.

Lin, D.C., Liu, C.H., Fang, T.H., Tsai, C.H., Murayama, M. and Chen, M.T., 2006, Millennial-scale changes in terrestrial sediment input and Holocene surface hydrography in the northern South China Sea (IMAGES ND972146). Paleogeography, Paleoclimatolology, Paleoecology, 236, 56-73.

Liu, Z., Colin, C., Li, X., Zhao, Y., Tuo, S., Chen, Z., Siringan, F.P., Liu, J.T., Huang, C.Y., You, C.F. and Huang, K.F., 2010, Clay mineral distribution in surface sediments of the northeastern South China Sea ad surrounding fluvial drainage basins: Source and transport. Marine Geology, 277, 48-60.

Mercer, J.L. and Zhao, M., 2004, Alkenone stratigraphy of the northern South China Sea for the past 35 M.Y., Sites 1147 and 1148, ODP Leg 184. Prell WL, Wang P, Blum P, Rea DK and Clemens SC (Eds.) Proceedings of the Ocean Drilling Program, Scientific Results Volume 184.

Nott, C.J., Xie, S., Avsejs, L.A., Maddy, D., Chambers, F.M. and Evershed, R.P., 2000, *n*-alkane distributions

in ombrotrophic mires as indicators of vegetation change related to climatic variation. Organic Geochemistry, 31, 231-235.

Pelejero, C., 2003, Terrigenous *n*-alkane input in the South China Sea: high-resolution records and surface sediments. Chemical Geology, 200, 89-103.

Pelejero, C. and Grimalt, J.O., 1997, The correlation between the U^{k}_{37} index and sea surface temperatures in the warm boundary: The South China Sea. Geochimica Cosmochimca Acta, 61, 4789-4797.

Pelejero, C., Grimalt, J.O., Heilig, S., Kienast, M. and Wang, L., 1999a, High resolution U^{k}_{37} temperature reconstruction in the South China Sea over past 220 kyr. Paleoceanography, 14, 224-231.

Pelejero, C., Grimalt, J.O., Sarnthein, M., Wang, L. and Flores, J.A., 1999b, Molecular biomarker record of sea surface temperature and climatic change in the South China Sea during the last 140,000 years. Marine Geology, 156, 109-121.

Petersen, H.I., Nytoft, H.P., Ratansathien, B. and Foopatthankamol, A., 2007, Oils from Cenozoic rift-basins in central and northern Thailand: source and thermal maturity. Journal of Petrological Geology, 30, 59-78.

Poynter, J.G., Farrimond, P., Robinson, N. and Eglinton, G., 1989, Aeolian-derived higher plant lipids in the marine sedimentary record: links with paleoclimate. In: Leinen M, Sarnthein M (Eds.), Paleoclimatology and paleometeorology: modern and past patterns of global atmospheric transport. Kluwer Academic Publisher, Dordrecht, The Nerherlands, 453-462.

Prahl, F.G., Muehlhausen, L.A. and Zahnle, D.L., 1988, Further evaluation of long-chain alkenones as indicators of paleoceanographic conditions. Geochimica et Cosmochimica Acta, 52, 2303-2310.

Prahl, F.G. and Wakeham, S.G., 1987, Calibration of unsaturation patterns in long-chain ketone compositions for paleotemperature assessment. Nature, 330, 367-369.

Sicre, M.A., Bard, E., Ezat, U. and Rostek, F., 2002, Alkenone distributions in the North Atlantic and Nordic sea surface waters. Geochemistry, Geophysics, Geosytems, 3, http://doi.org/10.1029/2001GC000159.

Sikes, E.L., Uhle, M.E., Nodder, S.D. and Howard, M.E., 2009, Sources of organic matter in a coastal marine environment: Evidence from *n*-alkane and their $\delta^{13}C$ distributions in the Hauraki Gulf, New Zealand. Marine Chemistry, 113,149-163.

Sikes, E.L., Volkman, J.K., Robertson, L.G. and Pichon, J.J., 1997, Alkenones and alkenes in surface water and sediments of the Southern Ocean: Implications for paleotemperature estimation in polar regions. Geochimica et Cosmochimica Acta, 61,1495-1505.

Street, J.H., Anderson, R.S., Rosenbauer, R.J. and Paytan, A., 2013, *n*-alkane evidence for the onset of wetter conditions in the Sierra Nevada, California (USA) at the mid-late Holocene transition, ~3.0 ka. Quaternary Research, 79, 14-23.

Sun, X., Li, X., Luo, Y. and Chen, X., 2000, The vegetation and climate at the last glaciation on the emerged continental shelf of the South China Sea. Paleogeography, paleoclimatology, Paleoecology, 160, 301-306.

Wan, S., Li, A., Clift, P.D. and Jiang, H., 2006, Development of the East Asian summer monsoon: Evidence from the sediment record in the South China Sea since 8.5 Ma. Paleogeography, Paleoclimatology, Paleoecology, 241, 139-159

Wang, P. and Li, Q., 2009, The South China Sea: Paleoceanography and Sedimentology. Vol. 13. (Eds.) Springer, 506 p.

Wang, P., Li, Q., Tian, J., He, J., Jian, Z., Ma, W. and Dang, H., 2016, Monsoon influence on planktic $\delta^{18}O$ records from the South China Sea. Quaternary Science Review, 142, 26-39.

Wang, P., Li, Q., Tian, J., Jian, Z., Liu, C., Li, L. and Ma, W.T., 2014, Long-term cycles in the carbon reservoir of the Quaternary Ocean: a perspective from the South China Sea. Nation Science Review, 1, 119-143.

Yamamoto, S., Kawamura, K., Seki, O., Meyers, P.A., Zheng, Y. and Zhou, W., 2010, Environmental influences over the last 16 ka on compound-specific $\delta^{13}C$ variations of leaf wax n-alkanes in the peat deposit from northeast China. Chemical Geology, 277, 261-268.

Yokoyama, Y., Naruse, T., Ogawa, N.O., Tada, R., Kitazato, H. and Ohkouchi, N., 2006, Dust influx reconstruction during the last 26,000 years inferred from a sedimentary leaf wax record from the Japan Sea. Global and Planetary Change, 54, 239-250.

Zhao, M., Huang, C.Y., Wang, C.C. and Wei, G., 2006, A millennial-scale Uk'_{37} sea-surface record from the South China Sea (8°N) over the last 150 kyr: Monsoon and sea-level influence. Paleogeography, Paleoclimatology, Paleoecology, 236, 39-55.

Zhou, B., Zheng, H.B., Yang, W.G., Taylor, D., Lu, Y.H., Wei, G.J., Li, L. and Wang, H., 2012, Climate and vegetation variations since the LGM recorded by biomarkers from a sediment core in the northern South China Sea. Journal Quaternary Science, 27, 948-955.

Received : October 28, 2021
Revised : February 14, 2022
Accepted : February 16, 2022